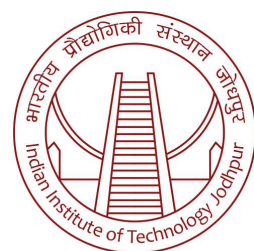


# Theoretical Investigations of Unimolecular and Bimolecular Reaction Dynamics in Gas Phase

*A Thesis submitted by*  
**Erum Gull Naz**

*in partial fulfillment of the requirements for the award of the degree of*  
**Doctor of Philosophy**



॥ त्वं ज्ञानमयो विज्ञानमयोऽसि ॥

**Indian Institute of Technology Jodhpur**  
**Department of Chemistry**  
*February 2021*



## Declaration

I hereby declare that the work presented in this Thesis titled ” *Theoretical Investigations of Unimolecular and Bimolecular Reaction Dynamics in Gas Phase*” submitted to the Indian Institute of Technology Jodhpur in partial fulfilment of the requirements for the award of the degree of Doctor of Philosophy, is a bonafide record of the research work carried out under the supervision of Dr. Manikandan Paranjothy. The contents of this thesis in full or in parts, have not been submitted to, and will not be submitted by me to, any other Institute or University in India or abroad for the award of any degree or diploma.



Erum Gull Naz  
P14CHM001



## Certificate

This is to certify that the thesis titled "*Theoretical Investigations of Unimolecular and Bimolecular Reaction Dynamics in Gas Phase*", submitted by Erum Gull Naz (P14CHM001) to the Indian Institute of Technology Jodhpur for the award of the degree of *Doctor of Philosophy*, is a bonafide record of the research work done by her under my supervision. To the best of my knowledge, the contents of this report, in full or in parts, have not been submitted to any other Institute or University for the award of any degree or diploma.

Dr. Manikandan Paranjothy  
Ph.D.Thesis Supervisor



# Abstract

For decades, classical trajectory simulations have been used to determine reaction mechanisms, energy flow pathways, product branching ratio, etc. Though atoms and molecules are quantum mechanical in nature, classical mechanics is used because of the inherent computational complexities associated with full quantum dynamics calculations. In a classical trajectory simulation, Newton's or Hamilton's equations of motion are time evolved using an appropriately selected set of initial coordinates and momenta. The time propagated coordinates and momenta are used to compute final properties of the system. A crucial aspect of trajectory integrations is selecting an appropriate potential energy surface. Conventionally, this is done with model potentials (classical force fields) and such calculations are fast but limited by accuracy. With the advancements in parallel computing techniques and sophisticated algorithms, it is possible to compute the required potentials and gradients (for trajectory integration) from a suitable electronic structure theory. Such an *on-the-fly* approach known as *direct dynamics* - is quite popular today and has led to identification of new mechanisms and pathways. Combining this method with electronic structure calculations, few unimolecular and bimolecular reactions were modeled in the present work. Selected reactions are of interest in combustion and interstellar chemistry.

The first reaction investigated was the bimolecular collision dynamics of  $\text{H}_3^+ + \text{CO}$  in the gas phase. The bimolecular reaction of  $\text{H}_3^+ + \text{CO}$  is one of the cornerstone chemical processes in the interstellar media. The products of this reaction are either formyl ( $\text{HCO}^+$ ) or isoformyl ( $\text{HOC}^+$ ) cation along with  $\text{H}_2$  molecule. These are barrier-less proton transfer and exoergic processes which results in the two isomers via ion-dipole complex formation. The reaction products are known to initiate the formation of important organic molecules in the interstellar media. Several experimental and theoretical investigations of the reaction probing structure and energetics, reaction mechanism, product branching ratios and  $\text{HCO}^+ \rightleftharpoons \text{HOC}^+$  isomerization have been reported. Ionic products of this reaction initiate different reaction networks in the interstellar media and their relative abundance in the space is a crucial quantity of interest. Direct dynamics simulations of  $\text{H}_3^+ + \text{CO}$  bimolecular reaction were performed using density functional PBE0/aug-cc-pVDZ level of theory to model a recently reported velocity imaging experimental studies of the same reaction. Reaction mechanisms, branching ratios, product energy and scattering angle distributions were computed from the trajectory data. Results are in qualitative agreement with experiments and detailed atomic level mechanisms are presented.

The second reaction studied was the unimolecular dissociation of  $\gamma$ -ketohydroperoxide (KHP).  $\gamma$ -ketohydroperoxide [(3-hydroperoxy)propanal] is an important reagent in synthetic chemistry. KHP is considered to be the primary source of radicals in low temperature combustion. Automated reaction discovery methods were utilized previously to study the unimolecular decomposition pathways of KHP. In the present work, direct chemical dynamics simulations at the B3LYP/6-31+G\* level of theory were performed to model the unimolecular decomposition of KHP identifying important dissociation pathways. Simulations were carried out at three different total energies mimicking thermal reaction conditions. Three dissociation channels among the previously reported pathways were identified to be important. Korcek decomposition, which was proposed earlier as a source of carbonyl compounds from thermal decomposition of KHP, was not observed in the present high-temperature simulations. However, trajectories showed the formation of carbonyl compounds such as aldehydes via other pathways. Further, Rice-Ramsperger-Kassel-Marcus (RRKM) rate constants were computed and compared with the trajectory data.

Thermal decomposition of thiophene, to understand the initial dissociation steps, were modeled at the B3LYP/6-31+G\* level of theory. Thiophene and its derivatives are present in the asphaltenes contained in oil shale and play an important role in the combustion reactions of alternative fuels. Electronic structure theory and experimental studies investigating the decomposition mechanisms of thiophene have been reported. In the present work, direct dynamics simulations were used to study the atomic level reaction mechanisms of gas phase pyrolysis of thiophene.



# Acknowledgments

I thank all who in one way or another contributed to the completion of this thesis. First, I give thanks to God for protection and the ability to do work.

I would like to thank all the people without whom this journey would never have been possible. Although it is just my name on the cover, many people have contributed to the research in their own particular way and for that, I want to give them special thanks.

First, my supervisor **Dr. Manikandan Paranjothy**, you have created the invaluable space for me to do this research and develop myself as a researcher in the best possible way. I greatly appreciate the freedom you have given me to find my own path and the guidance and support you offered when needed. Your mix of straightforward criticism combined with heart-warming support has given me great confidence as a researcher, and at the same time made me realize that I am only a beginner in this exciting profession.

I also want to thank my committee members, Dr. Samanwita Pal, Dr. Atul Kumar, and Dr. Satyajit Sahu. Thank you for investing time and providing interesting and valuable feedback. I feel proud and honored that you have accepted to be on my committee.

I thank all the faculty members of the Department of Chemistry for their support, and for improving my teaching skills through various experimental and theoretical courses. I am overwhelmed with your support and the excellent environment you have provided in the department. I would also like to thank IIT Jodhpur for providing proper infrastructure and research facilities in the institute.

I also thank Yogesh, your work has formed the basis for my research. Your help and support motivate me throughout my Ph.D. work. Thank you for all your feedback and encouragement. I would like to express my special appreciation and thanks to my friends Arpita Srivastava, Manju Kumari, Bhawna Chaubey, Hitesh Sharma, Parmod Kumar Paul, Rakesh Kumar, C.P.Goswami. A crucial ingredient in my work has been the rewarding interactions with my fellow Ph.D. labmates Anchal Gahlaut, Sumitra Godara, Himani Priya, and Akash Popat Gural.

I would like to thank Mr. Anil Kumar, Mr. Dheerendra Yadav, Mr. Gaurav Nigam, Mrs. Rashmi Dhyami, Mr. Ganpat Chaudhary, Mrs. Apeksha Mathur, Mr. Shubham Pandey, Mr. Mahesh Kumar, Mr. Sandeep Gehlot, and Mrs. Swati Khushwaha for assisting me during non-academic work at the institute.

I also thank my parents, siblings for standing by my side during the tough times of my Ph.D. journey. There is no way to thank you for everything you have done for me. Simply, thanks for being always present and doing the (im)possible to keep me going further. Your permanent love and confidence in me have encouraged me to go ahead in my study and career. Specifically, I want to appreciate you for taking care of my son when I was studying. My lifeline (my son) Zaufishan Akhtar is my hope for the future, strength for the present. His smile always stimulates me and gives me the energy to pushup my limits. As to my sweet little boy, my love and longing for him are beyond words. He is the softest point of my heart. I am sorry for not being able to accompany or witness every step of his growing up in the first three years of his life.

Without the support of all the people, I would not have been able to complete my research. Thanks, everyone for being with me during this journey.

Erum Gull Naz



# Contents

	<i>Page</i>
<i>Preface</i>	<i>i</i>
<i>Acknowledgements</i>	<i>iii</i>
<i>Contents</i>	<i>v</i>
<i>List of Figures</i>	<i>vii</i>
<i>List of Tables</i>	<i>viii</i>
<i>List of Symbols</i>	<i>xiii</i>
<i>List of Abbreviations</i>	<i>xv</i>
<b>Chapter 1: Introduction</b>	<b>1</b>
1.1 Chemical Reaction Dynamics	1
1.2 Reactions in Gas Phase	1
1.3 Electronic Structure Calculations	3
1.3.1 Born-Oppenheimer Approximation	3
1.3.2 Density Functional Theory	4
1.4 Direct Dynamics	5
1.5 Present Work and Organization of Thesis	6
<b>Chapter 2: Theoretical Methods and Techniques</b>	<b>7</b>
2.1 Electronic Structure	7
2.1.1 Features of PES	7
2.2 Automated Reaction Path Discovery Methods	9
2.2.1 Normal Mode Analysis	9
2.3 Born-Oppenheimer Direct Dynamics	10
2.3.1 Trajectory Initial Conditions	11
2.3.2 Integrator	12
2.3.3 Bimolecular Collisions	14
2.3.4 Unimolecular Dissociation Reactions	14
2.4 RRKM calculations	15
2.5 Software	15
<b>Chapter 3: Bimolecular Collision Dynamics of H<sub>3</sub><sup>+</sup> + CO Reaction</b>	<b>17</b>
3.1 Methodology	18
3.2 Potential Energy Profile	19
3.3 Simulation Results	19
3.3.1 Reactivity and Branching Ratio	19
3.3.2 Product Energy Distributions	22
3.3.3 Scattering Angles	24
3.4 Discussion	24
3.5 Summary	28
<b>Chapter 4: Unimolecular Dissociation of <math>\gamma</math>-Ketohydroperoxide</b>	<b>31</b>
4.1 Methodology and PES	32
4.2 Results and Discussion	34
4.2.1 Homolytic Dissociations	34
4.2.2 Malondialdehyde Channel	38
4.2.3 Acrolein Channel	38
4.2.4 Minor Channels	38
4.3 Discussion	41
4.4 Summary	43
<b>Chapter 5: Thermal Decomposition of Thiophene</b>	<b>45</b>
5.1 Methodology	46
5.2 Results	48
5.2.1 PES	48
5.3 Direct Dynamics	50
5.4 Summary	54
<b>Chapter 6: Summary</b>	<b>57</b>
<b>References</b>	<b>59</b>



# List of Figures

<i>Figure</i>	<i>Title</i>	<i>Page</i>
2.1	Potential energy surface[Schlegel, 2011], and its features.	8
2.2	Flowchart describing the steps involved in a classical trajectory simulation.	10
2.3	Numerical energy at each time step using a symplectic method and a non-symplectic Runge-Kutta method[Rieben <i>et al.</i> , 2004]. <i>y</i> axis shows energy in kcal/mol and <i>x</i> -axis shows time in units of $10^{-14}$ s.	12
3.1	$\text{H}_3^+ + \text{CO}$ Bimolecular Reaction	17
3.2	Potential energy profiles for (a) the bimolecular reaction $\text{H}_3^+ + \text{CO} \rightarrow \text{HCO}^+/\text{HOC}^+ + \text{H}_2$ and (b) the $\text{HCO}^+ \rightleftharpoons \text{HOC}^+$ isomerization reaction. Energies given are in units of kcal/mol and without zero point energy corrections. Also, zero point corrected energies are given in brackets.	19
3.3	Potential energy profiles for (a) the $\text{H}_3^+ + \text{CO} \rightarrow \text{HCO}^+/\text{HOC}^+ + \text{H}_2$ bimolecular reaction and (b) $\text{HCO}^+ \rightleftharpoons \text{HOC}^+$ isomerization reaction. Energies are given in units of kcal/mol without zero point energy corrections. Black lines correspond to density functional PBE0/aug-cc-pVDZ theory computed in the present work and blue lines correspond to benchmark CCSD(T)/CBS calculations taken from a previous work[Li <i>et al.</i> , 2008].	20
3.4	Optimized geometries of stationary points on the $[\text{H}_3\text{CO}]^+$ potential energy surface. The calculations were performed using the density functional PBE0/aug-cc-pVDZ level of theory. The bond lengths are given in units of Å. The numbers in brackets are bond lengths resulting from CCSD(T)/CBS benchmark calculations.	20
3.5	Total energy $E_{tot}$ as a function of integration time for several different classical trajectories.	21
3.6	Number of reactive trajectories (black circles), trajectories resulting in $\text{HCO}^+ + \text{H}_2$ (red squares), and $\text{HOC}^+ + \text{H}_2$ (blue triangles) as a function of relative energy $E_{rel}$ . The inset (black diamonds) shows branching ratios between $\text{HCO}^+$ and $\text{HOC}^+$ products as a function of $E_{rel}$ .	22
3.7	First row (from the top): normalized internal energy ( $E_{int} = E_{vib} + E_{rot}$ ) distributions of $\text{HCO}^+$ and $\text{HOC}^+$ products computed using all of the reactive trajectories. Second row: normalized $E_{int}$ distributions from only those trajectories satisfying the soft ZPE constraint. Third row: normalized and ZPE constrained $E_{int}$ distributions for only $\text{HCO}^+$ isomer. Fourth row: similar data for only $\text{HOC}^+$ isomer. The x-axes ranges are identical in all of the plots, and $E_{rel}$ is fixed for a given column.	23
3.8	(a)Trajectory averaged $\text{HCO}^+$ rotational energy ( $E_{rot}$ , blue squares), vibrational energy ( $E_{vib}$ , red triangles), and internal energy ( $E_{int}$ , black circles) plotted as a function of $E_{rel}$ . (b) Similar data but for $\text{HOC}^+$ . The insets in part a and b show similar data for $\text{H}_2$ . (c) Trajectory averaged fraction ( $f_{int}$ ) of total energy being transferred as internal energy to the ionic reaction products ( $\text{HCO}^+$ and $\text{HOC}^+$ ) is plotted as a function of $E_{rel}$ . The quantity $f_{int}$ is given for all scattering angles $\theta$ (black), trajectories with $\theta = 0-20^\circ$ (red), $\theta = 30-50^\circ$ (green), and $\theta = 60-80^\circ$ (blue).	24
3.9	Normalized product scattering angle distributions computed from $\text{HCO}^+$ trajectories, $\text{HOC}^+$ trajectories, and total reactive trajectories shown in the first, second, and third columns, respectively. $E_{rel}$ is the same in a given row. Respective axes ranges are the same in all of the plots.	25

3.10	Snapshots of trajectories (a) showing forward scattering at $E_{rel} = 2.7$ eV, (b),(c), and (d) showing isomerization at $E_{rel} = 4.3$ eV, (e) forming a $H_2...HOC^+$ complex before dissociation at $E_{rel} = 0.2$ eV, (f) forming $HOC^+$ initially and then resulting in $HCO^+$ via a roaming mechanism at $E_{rel} = 0.2$ eV. Relevant bond distances (in Å) as a function of time (in ps) are given in parts e and f. The number given inside each frame is the time (in fs) at which the snapshot was taken.	27
3.11	Snapshots and relevant bond distances of example trajectories showing different dynamical behavior at $E_{rel} = 0.2$ eV. Relevant bond distances (in Å) are given as a function of time (in ps). The number given inside each frame is the time (in fs) at which the snapshot was taken.	28
4.1	Total energy as a function of time for a few sample classical trajectories. In all plots, x-axes ranges are same y-axes show total energy in units of kcal/mol.	33
4.2	Dissociation energy profile of KHP computed using B3LYP/6-31+G* level of electronic structure theory. Energies are given in kcal/mol units and zero point energy not corrected.	34
4.3	Equilibrium geometries of reactant, products, and all the transition states computed using B3LYP/6-31+G* theory.	35
4.4	Numbering of backbone atoms of KHP used in the text for discussion purposes and the optimized geometries of TS1, TS3, and TS4.	35
4.5	Snapshots of example trajectories showing different KHP unimolecular reactions. (a) $KHP \rightarrow OH + HCHO + CH_2CHO$ , (b) $KHP \rightarrow H_2O + CO + CH_3CHO$ , and (c) $KHP \rightarrow H_2O + CH_2(CHO)_2 \rightarrow H_2O + CO + CH_3CHO$ . Number inside every frame is time in fs at which the snapshot was taken.	37
4.6	Snapshots of example trajectories. The numbers inside each panel is time in fs at which the snapshot was taken. Descriptions of the trajectories are given in the text.	40
4.7	Fraction of trajectories $f_T$ resulting in a particular product is shown for various observed reaction products at different total energies $E_{tot}$ .	42
4.8	Lifetime distributions computed from trajectories and RRKM theory are given as black circles and blue broken lines, respectively. The thick red lines show fit of trajectory data to sum of two exponential functions $N(t)/N(0) = f_1e^{-k_1t} + f_2e^{-k_2t}$ .	43
5.1	Dissociation energy profiles of thiophene computed using the B3LYP/6-31+G* level of electronic structure theory. Energies are given in kcal/mol units and are zero-point energy not corrected.	48
5.2	Equilibrium geometries of reactant, products, and intermediates of thiophene dissociation computed using B3LYP/6-31+G* theory.	49
5.3	Equilibrium geometries of all transition states associated with thiophene dissociation pathways computed using B3LYP/6-31+G* theory.	50
5.4	Total energy as a function of time for a few sample classical trajectories. In all plots, x-axes ranges are same y-axes show total energy in units of kcal/mol.	51
5.5	Description of initial steps of thiophene dissociation.	51
5.6	Snapshots of various trajectories showing different mechanisms. Numbers inside each frame is time in fs at which the snapshot was taken.	52
5.7	Snapshots of two example trajectories forming $CH_2CS + HCCH$ products (a) via IM6 formation and (b) direct ring dissociation. Numbers inside each frame is time in fs at which the snapshot was taken.	54

## List of Tables

<i>Table</i>	<i>Title</i>	<i>Page</i>
3.1	Summary of Trajectory Events Following $\text{H}_3^+ + \text{CO}$ Bimolecular Collision Reaction	21
3.2	Relative Energy Loss for the Two Isomer Channels	26
4.1	Stationary point energies (in kcal/mol) for the unimolecular dissociation of KHP computed using different levels of theory. The given values are relative to respective KHP energies and zero point energy not corrected.	33
4.2	Number of direct dynamics trajectories classified based on initial dissociation steps.	36
4.3	Number of trajectories resulting in various products following O(5)-O(6) and C(3)-C(4) dissociations.	37
4.4	Subsequent dissociation products of malondialdehyde channel.	38
4.5	Minor dissociation products of KHP unimolecular dissociation.	39
5.1	Stationary point energies (in kcal/mol) of the unimolecular dissociation of thiophene computed using different levels of theory. The given values are relative to respective thiophene energies and zero point energy not corrected.	47
5.2	Number of trajectories classified based on initial step for the 250 kcal/mol simulation. Description of the steps is shown in Figure 5.5.	51
5.3	Number of trajectories resulting in various reaction products following C-S dissociation accompanied by H transfer from C3 to C2.	53
5.4	Number of trajectories resulting in various reaction products following C-S dissociation.	54
5.5	Number of trajectories resulting in various reaction products.	55





## List of Symbols

$\text{\AA}$	Angstrom
fs	femtosecond
ps	picosecond
kcal/mol	kilo calorie per mole
eV	electronvolt
$\rho$	Electron probability density
$\psi$	Molecular wave function
$\psi_{el}$	Electronic wavefunction
$\vec{r}$	Electronic coordinates
$\vec{R}$	Nuclear coordinates
Z	Atomic number of nucleus
$\hat{H}$	Hamiltonian operator
V	Potential energy of the system
T	Kinetic energy of the system
q	Position of a particle
p	Momenta of a particle
rc	Reaction coordinate
$\nu$	Normal mode vibrational frequency
k	Force constant
$\mu$	Reduced mass of the molecule
t	Time
m	Mass
F	Force
$\Delta t$	Integration timestep

$k(E)$	RRKM rate constant
$E_{tot}$	Total energy
$E_{int}$	Internal energy
$E_{rot}$	Rotational energy
$E_{vib}$	Vibrational energy
$E_{rel}$	Relative energy
$b$	Collision Impact parameter
$\sigma_r$	Collision cross section
$v$	Relative velocity
$P_r(b)$	Reaction probability
$P(\theta)$	Scattering angle distribution
$f_t$	Fractions of trajectories
$k_B$	Boltzmann constant
$h$	Planck's constant
$T$	Temperature
H	Hydrogen
C	Carbon
O	Oxygen
S	Sulphur

## List of Abbreviations

BOMD	Born-Oppenheimer Molecular Dynamics
B3LYP	Becke, 3-parameter, Lee-Yang-Parr
CBS	Complete Basis Set
CC	Coupled Cluster
CCSD(T)	Coupled Cluster Single-Double and perturbative Triple
CPMD	Car-Parrinello molecular dynamics
DFT	Density Functional Theory
HF	Hartree-Fock
IM	Intermediate
IRC	Intrinsic Reaction Coordinate
IVR	Intramolecular Vibrational energy Redistribution
KHP	Ketohydroperoxide
MCTDH	Multi-configuration time-dependent Hartree
MP2	Møller-Plesset Perturbation theory of second-order
MM	Molecular Mechanics
NWChem	NorthWest Chemistry
PBE0	Perdew-Burke-Ernzerhof-0
PE	Potential Energy
PES	Potential Energy Surface
QM	Quantum Mechanics
RRKM	Rice-Ramsperger-Kassel-Marcus
TS	Transition State
TST	Transition State Theory
ZPE	Zero Point Energy

